Jahangirnagar University Environmental Bulletin, Vol. 10, 19-34, 2025

Jahangirnagar University Environmental Bulletin

ISSN: 2304-3326

Contents Available at: https://www.juniv.edu/department/env

Integrated Geostatistical and Deep Learning Approach for Groundwater Level Monitoring and Prediction in Savar Upazila, Bangladesh

Syed Hafizur Rahman[1*] and Mahfuzul Islam[2]

[1]*Proferssor, Department of Environmental Sciences, Jahangirnagar University, Savar, Dhaka-1342, Bangladesh.*

[2]*Graduate student, Department of Environmental Sciences, Jahangirnagar University, Savar, Dhaka-1342, Bangladesh.*

Abstract

Groundwater is an essential resource in Bangladesh, supporting both domestic consumption and agriculture. Rapid urbanization, industrialization, and geomorphological changes have led to a significant depletion of groundwater levels, particularly in areas like Savar Upazila. This study integrates spatial interpolation and machine learning approaches to assess and predict groundwater level fluctuations in Savar. Kriging, a geostatistical interpolation technique, was applied using groundwater data from five boreholes to map spatial distributions and identify zones of depletion. Results showed deeper groundwater levels in industrial zones such as Ashulia and Baipyle, whereas agricultural regions like Dhamrai exhibited shallower levels, likely due to greater groundwater recharge through wetlands. To forecast groundwater dynamics, a Long Short-Term Memory (LSTM) neural network model was developed using meteorological inputs (rainfall, evaporation, and runoff) alongside historical groundwater data. The model achieved high accuracy, with average training and validation losses of 0.013 and 0.010, respectively. Results from the five boreholes demonstrated the LSTM model's ability to effectively learn temporal patterns and predict groundwater levels with minimal error. This highlights the value of combining remote sensing, geostatistics, and deep learning for water resource management. The study emphasizes the importance of continuous groundwater monitoring, especially in rapidly developing urban-industrial landscapes. The integration of Kriging and LSTM modeling provides a robust framework for assessing and forecasting groundwater dynamics, offering valuable insights for sustainable water resource planning and climate adaptation strategies in Bangladesh and similar contexts.

Keywords: *Kriging Interpolation; LSTM Neural Network; Remote Sensing; Spatiotemporal Analysis*

Introduction

Groundwater is an essential element of the global hydrological cycle, functioning as a natural reservoir that accumulates and discharges water over time. Comprehending the dynamics of groundwater levels is crucial for sustainable water management, since it directly affects the availability of water for human consumption, agriculture, and ecosystem vitality. Globally, 99% of freshwater is derived from groundwater (Programme, 2022). In Bangladesh,

*Corresponding Author: hafizsr@juniv.edu

groundwater sources are critically significant for drinking water supply and the agricultural industry. Ninety-seven percent of drinking water is derived from groundwater, and agricultural activities during the dry season mostly rely on this groundwater supply (Shamsudduha, 2013). Geomorphologically, Bangladesh possesses a substantial reserve of aquifers from which groundwater can be readily collected throughout the year. The availability of groundwater sources, excessive extraction, and alteration of the natural landscape, which diminishes groundwater recharge points, ultimately leads to the depletion of groundwater levels (Islam and Mostafa, 2021). This poses a significant problem for human activities and the natural environment (Bierkens & Wada, 2019).

Traditionally, groundwater monitoring depended on sparse and localised well networks, frequently leading to restricted regional coverage and temporal resolution (Gibbons *et al.*, 2009). Historically, they depended on local well networks and hand measurements (Bhatti *et al.*, 2017; Einarson & Cherry, 2002; Quevauviller *et al.*, 2009). Conventional approaches are resource-demanding, time-intensive, and may inadequately encompass the intricate dynamics of aquifer systems. This has resulted in heightened interest in incorporating technologies and methodologies to improve the spatial and temporal scope of groundwater level evaluations. Technological advancements, especially in remote sensing and modelling techniques, have transformed our capacity to evaluate and forecast groundwater levels on a larger scale (Alshehri *et al.*, 2020; Brunner *et al.*, 2007; Khaki *et al.*, 2016; Usman *et al.*, 2020; Xu *et al.*, 2020). In regions such as Bangladesh, where effective management and advanced technologies are scarce, this methodology can be advantageous. This study intended to investigate the integration of remote sensing and modelling approaches for assessing and predicting groundwater levels to evaluate their relevance, applicability, and suitability for successful water resource management.

Spatial interpolation (Kriging)

The origins of Kriging can be attributed to the groundbreaking contributions of French mathematician Georges Matheron in the 1950s. Kriging, a geostatistical interpolation technique, has developed and gained extensive use across various domains like geology, hydrology, environmental science, and agriculture. Its prominence in groundwater level evaluation stems from its capacity to integrate the geographical configuration of the data, yielding solid estimates and dependable uncertainty assessments. Kriging fundamentally relies on the notion of regionalised variables, utilising the spatial correlation among sample points to estimate values at unobserved places. A notable characteristic of Kriging is its capacity to deliver both forecasts and measurable uncertainty assessments. This is essential in groundwater level evaluation, because decision-makers necessitate dependable information for sustainable water resource management. Kriging provides a comprehensive methodology for delineating the spatial variability of groundwater levels and generating maps that reflect the confidence in the projections (Oliver and Webster, 1990).

A multitude of studies has evidenced the efficacy of Kriging in global groundwater research. Nourani, Ejlali, and Alami (2011) utilised Kriging to evaluate groundwater levels in a coastal aquifer, uncovering intricate spatial patterns and facilitating the identification of probable over-extraction zones. Nas and Berktay (2010) employed Kriging to examine the spatial

distribution of groundwater levels in an urban setting, highlighting the technique's capacity to detect nuanced differences in groundwater dynamics.

Artificial neural network models

Artificial Neural Networks (ANNs) have emerged as a formidable instrument for modelling intricate hydrogeological systems, drawing inspiration from the architecture and operation of the human brain, and are computer models proficient in learning and adapting from input-output interactions (Yegnanarayana, 2009). Artificial Neural Networks (ANNs) have interconnected nodes, or neurones, arranged in layers, which include an input layer, hidden layers, and an output layer. The network acquires knowledge by modifying the weights of connections during a training period, allowing it to identify intricate non-linear correlations within the data (Abraham, 2005; Zou, Han, and So, 2008).

The typical artificial neural network (ANN) has some limitations. A fundamental shortcoming of the feed-forward neural network is its lack of memory retention. It is useful in static classification systems; but, in dynamic classification tasks, where the output relies on preceding timesteps, it fails to yield a correct response (Staudemeyer and Morris, 2019). Recurrent Neural Networks (RNNs) were created to address this issue by including signals from preceding timesteps (Rumelhart, Hinton, and Williams, 1986; Williams and Zipser, 1989; Werbos, 1990; Mozer, 1991). Traditional RNNs has limited memory capacity, resulting in the vanishing gradient problem. The fundamental architecture of Artificial Neural Networks (ANN) and Recurrent Neural Networks (RNN) is depicted in Figure 1.

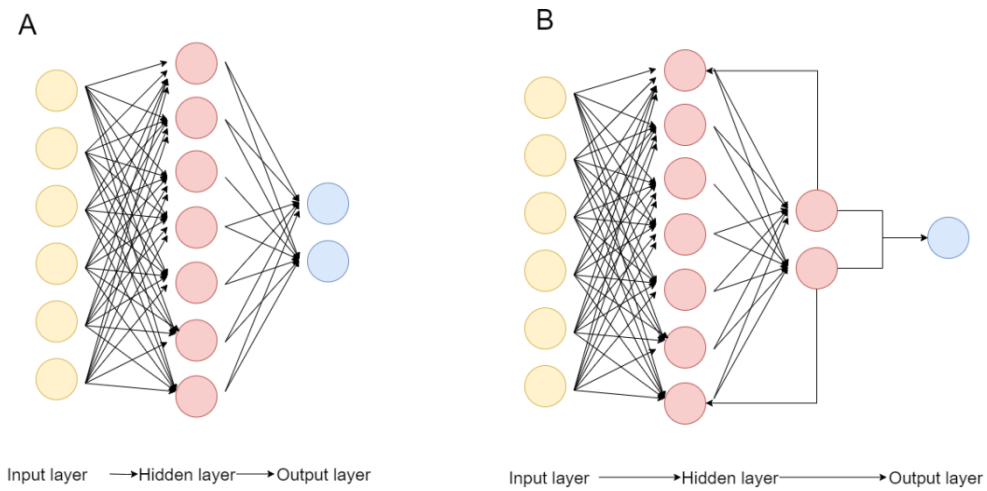

Figure 1: (A) Basic architecture of an artificial neural network, ANN, (B) Basic architecture of a recurrent neural network, RNN

Long Short-Term Memory (LSTM)

LSTMs are a kind of RNNs formulated to mitigate the vanishing gradient issue that may arise in conventional RNNs during the acquisition of long-term dependencies. LSTMs

utilise memory cells to save information throughout extended sequences (Hochreiter & Schmidhuber, 1997; Gers, Schmidhuber & Cummins, 2000; Pérez-Ortiz *et al.*, 2003; Indermühle *et al.*, 2011; Yu *et al.*, 2019). Utilising the memory cell design, LSTMs can judiciously retain or discard information over time, guaranteeing that prior observations suitably influence future predictions (Hochreiter and Schmidhuber, 1997). This adaptive memory process is especially beneficial for estimating groundwater levels, as historical data is essential for identifying seasonality, trends, and other long-term patterns (Graves, 2012). The intrinsic characteristics of LSTM networks render them a dependable and effective option for precise groundwater level forecasting, thereby enabling informed decision-making in water resource management and environmental planning (Alshehri *et al.*, 2020; Sit *et al.*, 2020). Numerous instances exist about LSTM-related challenges associated with groundwater levels. Nourani, Khodkar, and Gebremichael (2022) employed LSTM for the uncertainty evaluation of groundwater levels, while Vu *et al.* (2020) utilised LSTM to rebuild absent groundwater level data.

This study aimed to evaluate the groundwater level of Savar Upazila using remote sensing technologies and interpolation techniques, followed by an analysis of historical data to develop an artificial neural network model for predicting future water level fluctuations.

Materials and Methods

Study area

The designated research area is Savar Upazila, located in Bangladesh, with coordinates extending from 90°15'5.193"E, 24°1'59.417"N to 90°19'59.534"E, 23°44'27.116"N in the north-south direction, and from 90°10'55.066"E, 24°0'15.829"N to 90°21'22.909"E, 23°52'29.683"N in the east-west direction (Figure 2). Savar, located in the Dhaka district, is bordered by five upazilas: Dhamrai and Shingair to the west, Keraniganj to the south, Dhaka and Tongi to the east, and Kaliakoir to the north.

The entire land area of Savar Upazila is 280.12 km² (Bangladesh, 2023). The upazila is encircled by three rivers: the Bangshal, the Turag, and the Dhaleshwari. Approximately 18,000 hectares of land are utilised for agricultural purposes. Approximately 1,200 small to major industries are located throughout the region.

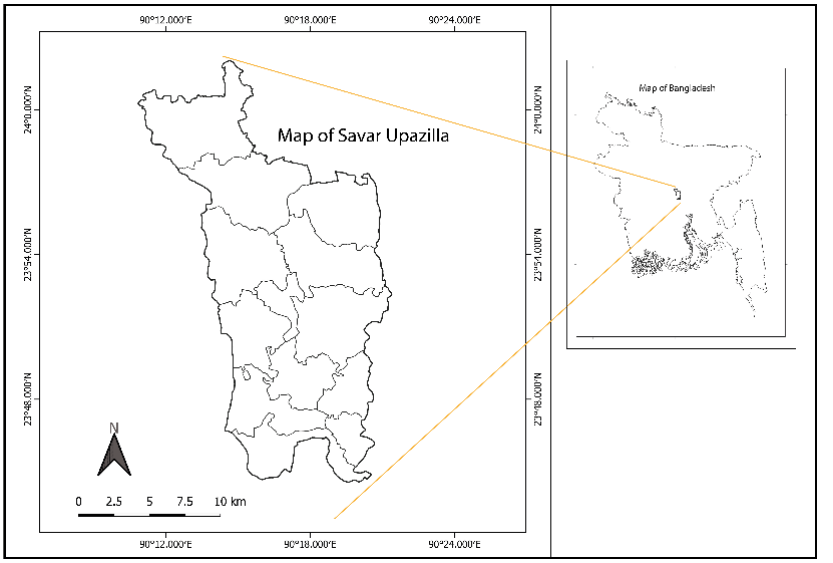

Figure 2: Study area map.

A summary of the methodology is shown in Figure 3.

Figure 3: Summary of the Methodology.

Data collection

Groundwater level data, collected weekly from five distinct boreholes in the research area, were obtained from the Bangladesh Water Development Board (BWDB) for the kriging analysis and LSTM prediction (Figure 4 and Table 1). Three categories of meteorological data (precipitation, total surface runoff, and total evaporation) were gathered for the study. All data were obtained from the timeframe of 2008 to 2017 (Table 2).

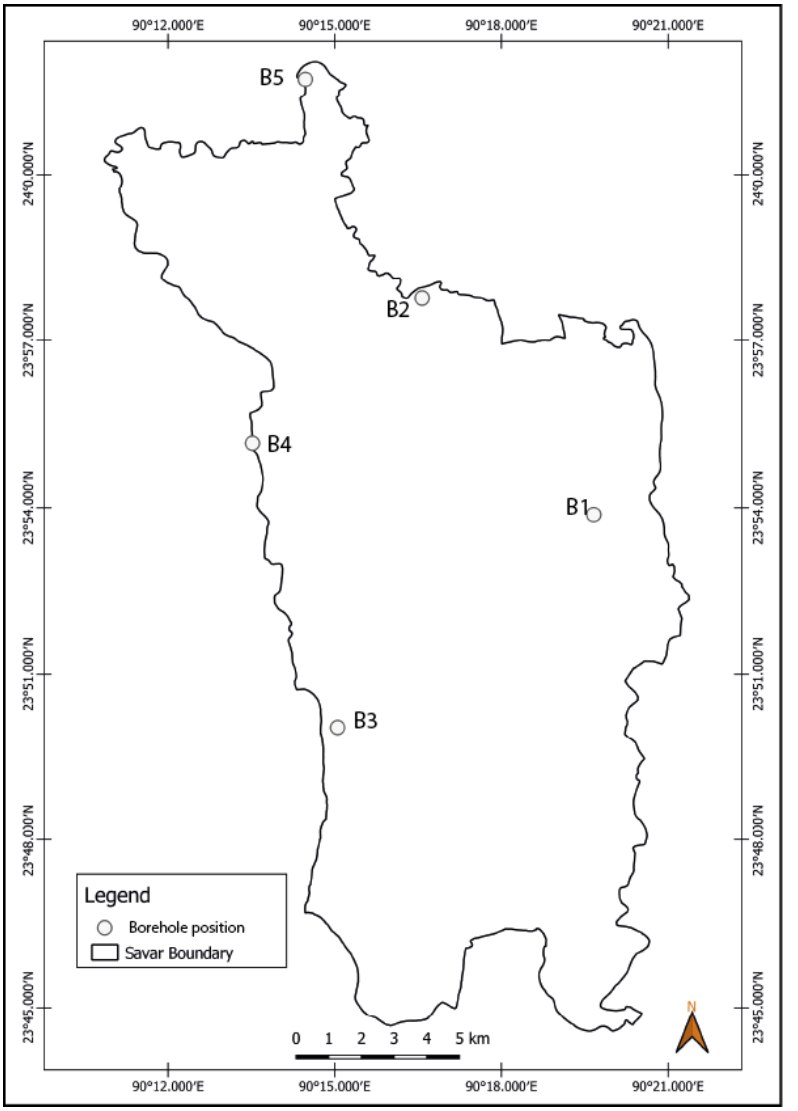

Figure 4: Borehole data collection points.

Table 1: Details about the boreholes, their positions, and timescale

Id	Name of place	Position (Coordinate)	Timescale
B1	Ashulia	90.33422,23.89747	2012-2017
B2	Baipyle	90.27524,23.94227	2008-2017
B3	Savar	90.25085,23.83452	2008-2017
B4	Dhamrai	90.22476,23.91959	2008-2017
B5	Konabari	90.24064,24.02904	2008-2017

Table 2: Details about the other meteorological data

Type	Source	Timescale	Frequency
Rainfall data	CHIRPS Pentad	2008-2017	Daily
Total Evaporation	ERA5-Land Daily Aggregated	2008-2017	Daily
Total surface runoff	ERA5-Land Daily Aggregated	2008-2017	Daily

Tools and materials

Quantum GIS 3.22 was utilised for the preparation of remote and geographical data. Kriging analysis was conducted using ArcGIS 10.8 software. The artificial neural network and data filtration and sorting were constructed using Python. The Anaconda environment was utilised for model creation and execution. All these tasks have been executed on a PC equipped with a 12th generation Core i7 CPU.

Kriging analysis

Groundwater level data were systematically collected from five boreholes located in Savar Upazila. Data obtained for each borehole encompassed exact geographic coordinates (latitude and longitude), elevation above mean sea level, and groundwater levels at many intervals, so establishing a comprehensive dataset for spatial analysis. The data preparation included a comprehensive evaluation of the borehole coordinates for precision and the standardisation of measurement units across all data points. The groundwater level data were transformed into a structured database compatible with ArcGIS, enabling simple integration into the Spatial Analyst tool for further study. The Spatial Analyst tool in ArcGIS provides an extensive array of functionalities for conducting sophisticated geospatial studies, including Kriging interpolation, which was the principal technique utilised to estimate groundwater levels in unsampled regions of Savar Upazilla (Childs, 2004). The actions executed were as follows:

Spatial Analyst Tool Configuration: The study commenced with the configuration of the ArcGIS project to integrate the Spatial Analyst extension, thereby facilitating access to advanced spatial interpolation methods, including the Kriging tool.

Exploratory Spatial Data Analysis (ESDA): An exploratory analysis was performed to comprehend the spatial attributes and distribution of the gathered groundwater level data. This stage was essential for discerning geographical patterns, trends, and the extent of spatial autocorrelation in the dataset, which directly affects the selection of the Kriging model and its parameters (Haining *et al.*, 1998).

Selection of Kriging Models: Utilising insights from ESDA, the Kriging tool was employed to identify the optimal Kriging model (Ordinary Kriging) for the dataset. This selection was guided by the identified spatial patterns and autocorrelation.

Executing Kriging Interpolation: Employing the Spatial Analyst's Kriging tool, groundwater levels at unmeasured places were estimated, generating a continuous surface that illustrates the spatial distribution of groundwater levels throughout Savar Upazila. This interpolation took into account the variogram model parameters to guarantee that the predictions were unbiased and exhibited low variance.

LSTM analysis

This project seeks to create a Long Short-Term Memory (LSTM) neural network model for predicting groundwater levels in Savar upazila, an essential endeavour in water resource management and environmental planning. The methodology includes data collection, preprocessing, model architecture design, training, assessment, and result interpretation.

Data Sanitisation

The objective of this section was to eliminate absent or inaccurate data entries to preserve the integrity of the model's input. The basic dataset of groundwater levels and other data exhibits varying frequencies, specifically weekly and daily; thus, it was necessary to standardise the data frequency. The task was executed using Python coding in Jupyter Notebook. The 'Pandas' library was utilised to develop the code. The 'parser' submodule from the 'dateutil' module was utilised to interpret the date (dateutil, 2019). This code generated a CSV file encompassing rainfall data, runoff data, and total evaporation data aligned with the dates of water level data within a singular sheet.

Design of Model Architecture

The dataset utilised in this analysis is derived from the preceding section, encompassing a defined time range and comprising variables such as precipitation, evaporation, surface runoff, and groundwater levels. Preprocessing stages encompass data cleansing to address absent values, outliers, and anomalies. Relevant features affecting groundwater levels are chosen, and Min-Max scaling is utilised to normalise the features and target variable, facilitating model convergence. Normalisation is executed with MinMaxScaler to adjust data within the range of 0 to 1.

The LSTM model architecture is meticulously crafted to incorporate temporal dependencies in the sequential groundwater level data (Figure 5). This overview presents the LSTM architecture, highlighting its capacity to preserve information throughout extended durations and address vanishing gradient issues. The model configuration comprises an input layer that accommodates feature sequences over a specified time window, three hidden LSTM layers utilising suitable activation functions (e.g., ReLU and tanh) (Banerjee *et al.*, 2019), and a sigmoid activation function in the output layer for predicting groundwater levels (Sharma *et al.*, 2017). Hyperparameters, including the quantity of LSTM units, batch size, learning rate, and number of epochs, are determined through testing and validation.

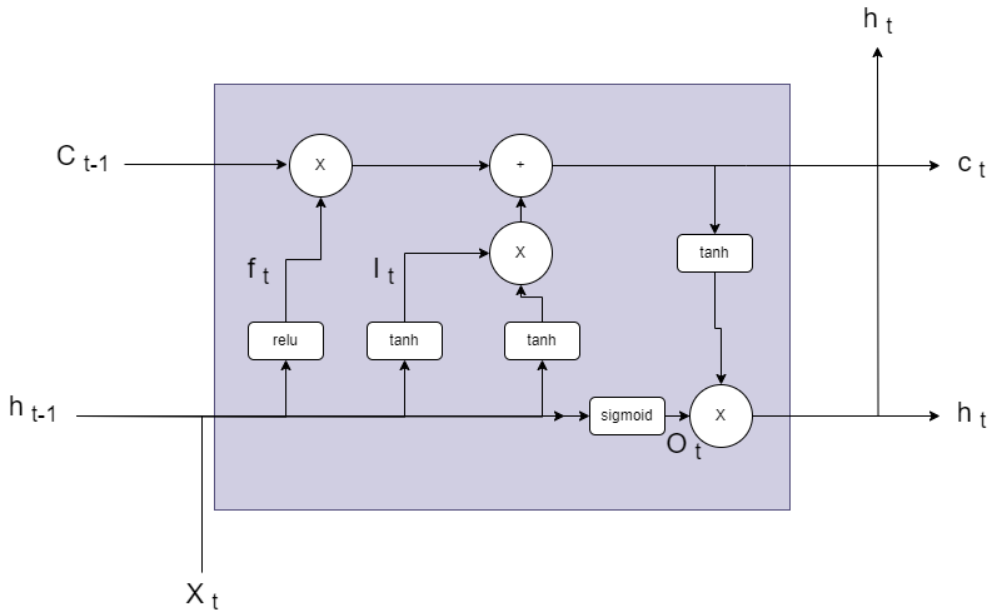

Figure 5: Architecture of the LSTM model.

The dataset is partitioned into training and testing sets for model training, maintaining temporal continuity. The LSTM model is constructed using a suitable loss function, such as mean squared logarithmic error, and an optimiser, such as Adam (Oppermann, 2022). The training process entails the iterative modification of model parameters to reduce the loss function on the training dataset, while simultaneously observing convergence and validation efficacy.

Model evaluation utilises performance indicators like mean squared error, mean absolute error, and the coefficient of determination (R^2). Visualisations, such as charts comparing actual and forecast groundwater levels, are employed to evaluate model accuracy and generalisation. The results and discussion emphasise the efficacy of the LSTM model, the obstacles faced during training, and possible pathways for enhancement. Inclusion of comparative analysis with baseline models or alternative forecasting methodologies may be warranted if relevant.

Model evaluation entails analysing the training and validation loss curves to verify convergence and identify overfitting. Line plots are utilised to visualise the comparison between actual and expected groundwater levels, juxtaposing the model's forecasts with the true values from the test set.

The execution occurred within a Jupyter Notebook environment utilising the TensorFlow and Keras frameworks for model construction and pandas for data preprocessing (Gulli & Pal, 2017; Ketkar & Ketkar, 2017; McKinney, 2012; McKinney & Team, 2015; Pang *et al.*, 2020).

Results

Interpolation

The interpolation of groundwater levels from five boreholes suggests that the region including Ashulia, Baipyle, and Kaliakoir exhibits the greatest depth of groundwater level, signifying substantial upwelling of water (Figure 6). Furthermore, these regions are predominantly industrial zones where the majority of enterprises depend on groundwater for production and processing activities. This elucidates the cause of the depletion of the GWL. Conversely, the region adjacent to Dhamrai and Noyar exhibits the minimum depth of groundwater level. These regions are predominantly agricultural grounds. Despite the substantial extraction of groundwater from this region, it also contains several recharge zones for groundwater via wetlands, which are rather scarce in industrial areas.

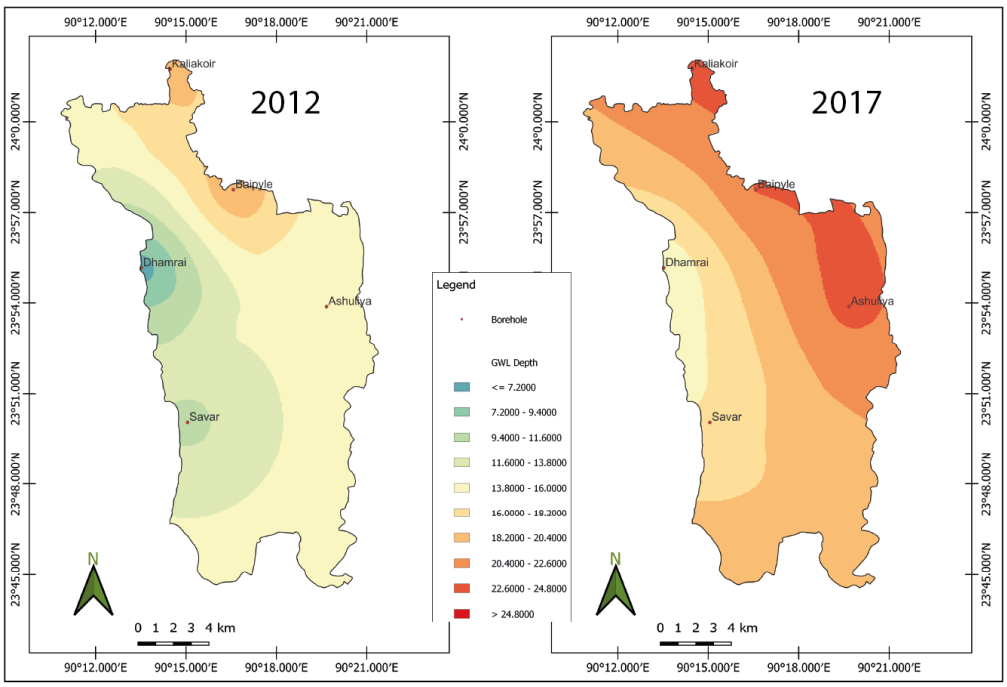

Figure 6: Interpolation maps of Savar Upazilla GWL from 2012 to 2017.

GWL Prediction

The main aim of this study was to create a Long Short-Term Memory (LSTM) artificial neural network (ANN) to forecast groundwater levels using recorded rainfall, runoff, and evaporation data. We systematically created, trained, and assessed a model in accordance with the previously outlined methodology. Five distinct operations have been conducted on five borehole datasets.

Forecast for Ashulia

The model architecture comprised an input layer for three features (rainfall, surface runoff, and evaporation), three hidden layers containing 247, 100, and 50 neurones respectively, utilising ReLU activation for the first hidden layer and tanh activation functions for the subsequent two layers to capture nonlinear relationships. A concluding dense layer with a sigmoid activation method generates expected groundwater levels. The Adam optimiser is selected for model training because of its efficacy in managing sparse gradients and noisy data. The learning rate is established at 0.001.

The dataset is divided into training and testing subsets (80-20 ratio), and the LSTM model is trained for 500 epochs with a batch size of 8, incorporating a 10% validation split for performance evaluation. The training loss was 0.000287 while the validation loss was 0.0070. Figure 7 illustrates the expected groundwater level in comparison to the actual data.

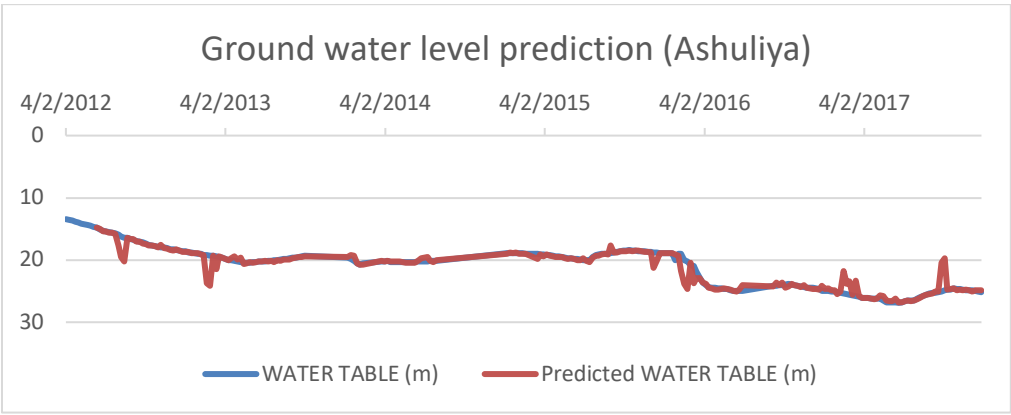

Figure 7: Groundwater level prediction vs real-life data for Ashuliya.

Forecast for Baipyle

The model architecture included an input layer for three features (rainfall, surface runoff, and evaporation), three hidden layers with 316, 100, and 50 neurones respectively, employing ReLU activation for the first hidden layer and tanh activation functions for the subsequent two layers to capture nonlinear relationships. A concluding dense layer utilising a sigmoid activation method generates expected groundwater levels. The Adam optimiser is selected for model training because of its efficacy in managing sparse gradients and noisy data. The learning rate is established at 0.001.

The dataset is divided into training and testing sets in an 80-20 ratio, and the LSTM model is trained for 500 epochs with a batch size of 16, employing a 10% validation split for performance evaluation. The training loss was 0.0089, while the validation loss was 0.0059. Figure 8 illustrates the projected groundwater level compared to the actual data.

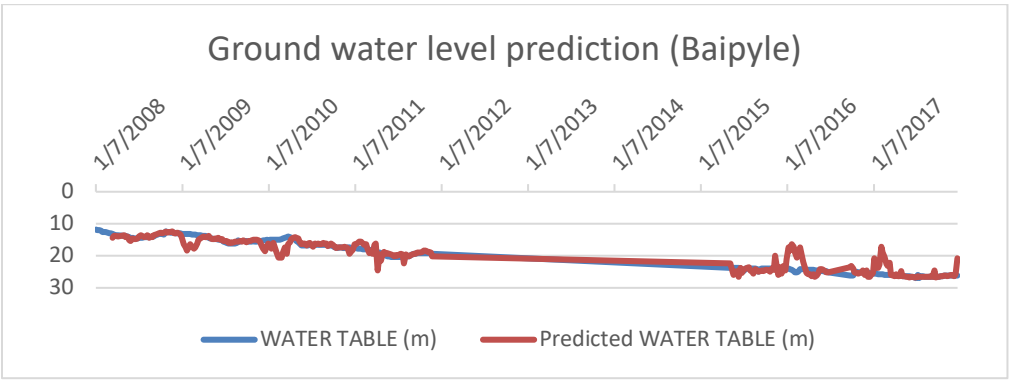

Figure 8: Groundwater level prediction vs real-life data for Baipyle.

Forecast for Savar

The model architecture included an input layer for three features (rainfall, surface runoff, and evaporation), three hidden layers with 487, 100, and 50 neurones respectively, utilising ReLU activation for the first hidden layer and tanh activation functions for the subsequent two layers to capture nonlinear relationships. A concluding dense layer with a sigmoid activation method generates expected groundwater levels. The Adam optimiser is selected for model training because of its efficacy in managing sparse gradients and noisy data. The learning rate is established at 0.001.

The dataset is divided into training and testing subsets (80-20 ratio), and the LSTM model is trained for 325 epochs with a batch size of 32, employing a validation split of 10% for performance evaluation. The training loss was 0.0014, whereas the validation loss was 0.005. Figure 9 illustrates the expected groundwater level in comparison to the actual data.

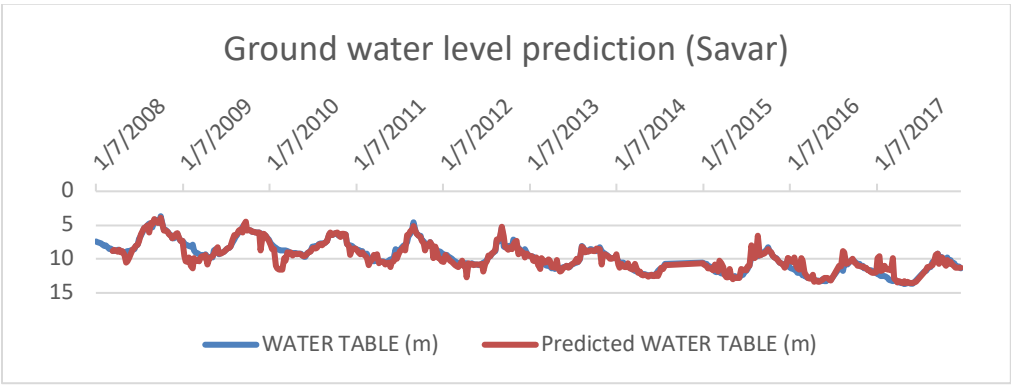

Figure 9: Groundwater level prediction vs real-life data for Savar.

Forecast for Dhamrai

The model architecture comprised an input layer for three features (rainfall, surface runoff, and evaporation), three hidden layers containing 470, 100, and 50 neurones respectively, utilising ReLU activation for the first hidden layer and tanh activation functions for the subsequent two layers to capture nonlinear relationships. A terminal dense layer employing a sigmoid activation algorithm generates projected groundwater levels. The Adam optimiser is selected for model training because of its efficacy in managing sparse gradients and noisy data. The learning rate is established at 0.001.

The dataset is divided into training and testing sets in an 80-20 ratio, and the LSTM model is trained for 200 epochs with a batch size of 16, employing a 10% validation split for performance evaluation. The training loss was 0.000303, while the validation loss was 0.0098. Figure 10 illustrates the expected groundwater level in comparison to the actual data.

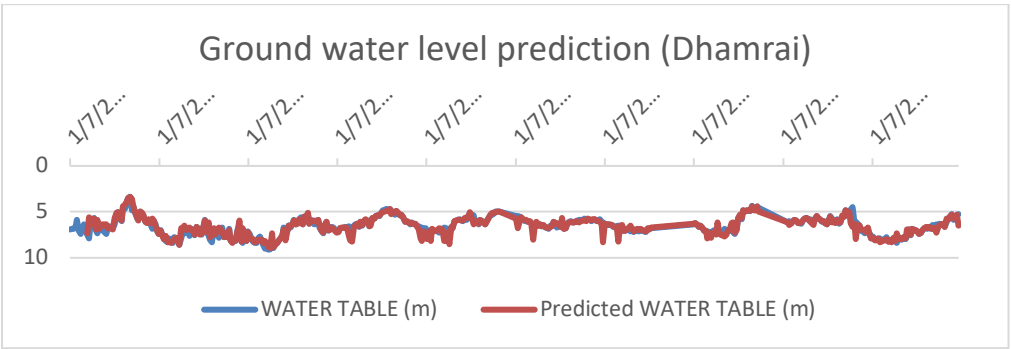

Figure 10: Groundwater level prediction vs real-life data for Dhamrai.

Forecast for Kaliakoir

The model architecture included an input layer for three features (rainfall, surface runoff, and evaporation), three hidden layers with 360, 100, and 50 neurones respectively, utilising ReLU activation for the first hidden layer and tanh activation functions for the subsequent two layers to capture nonlinear relationships. A concluding dense layer utilising a sigmoid activation method generates expected groundwater levels. The Adam optimiser is selected for model training because of its efficacy in managing sparse gradients and noisy data. The learning rate is established at 0.01.

The dataset is divided into training and testing sets in an 80-20 ratio, and the LSTM model is trained for 500 epochs with a batch size of 16, utilising a 10% validation split for performance evaluation. The training loss was 0.0030, while the validation loss was 0.023. Figure 11 illustrates the expected groundwater level in comparison to the actual data.

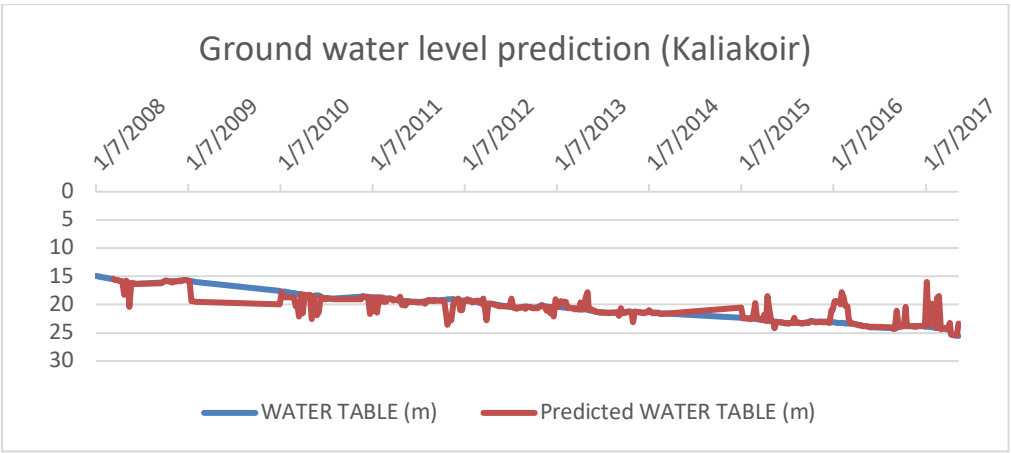

Figure 11: Groundwater level prediction vs real-life data for Kaliakoir.

Conclusion

The interpolation results obtained by Kriging indicate the water-scarce region of Savar. The majority of locations within industrial and residential zones exhibit a significant depth of groundwater level. Conversely, the location of the agricultural areas exhibits a shallow groundwater level. This finally signifies the reduced permeability of water in metropolitan regions.

The model attained an average training loss of 0.013 and an average validation loss of 0.010. This outcome signifies a minimal error rate in the model's forecasts of groundwater levels, indicating that the model has effectively delineated the intrinsic link among rainfall, evaporation, and groundwater levels. The comparatively minimal test loss indicates the effectiveness of the ANN in comprehending and forecasting groundwater level changes with considerable precision.

A training loss of 1.3% and a validation loss of 1% indicate the model's strong prediction accuracy. In groundwater level prediction, where accuracy is essential for planning and management, this outcome underscores the potential of artificial neural networks to provide significant insights into water resource management strategies. It emphasises the significance of choosing suitable model topologies, training periods (epochs), and preprocessing methods to enhance model performance.

Savar has both urban and rural areas, featuring significant portions experiencing swift industrialisation and urbanisation while retaining a rural identity. The regions of Ashulia, Jirabo, Baipyle, and Hemayatpur have witnessed considerable industrial expansion, whereas Savar Pauroshova, Bank Town, Birulia, and other locales have experienced major urban development. In contrast, areas next to the Dhamrai Upazilla maintain a rural atmosphere.

The diverse terrain of Savar creates a spectrum of water requirements. Groundwater constitutes the principal water source in this region, underscoring the necessity of monitoring and assessing fluctuations in groundwater levels.

Acknowledgement

For funding the study during the 2024–2025 fiscal year, the authors would like to thank Jahangirnagar University's Faculty of Mathematical and Physical Sciences.

References

Abraham, A. (2005) 'Artificial Neural Networks', *Handbook of Measuring System Design* [Preprint]. Available at: https://doi.org/10.1002/0471497398.MM421.

Alshehri, F. *et al.* (2020) 'Mapping the distribution of shallow groundwater occurrences using remote sensing-based statistical modeling over southwest Saudi Arabia', *Remote Sensing*, 12(9). Available at: https://doi.org/10.3390/RS12091361.

dateutil (2019) *parser — dateutil 3.9.0 documentation*, *https://dateutil.readthedocs.io/en/stable/parser.html*. Available at: https://dateutil.readthedocs.io/en/stable/parser.html (Accessed: 14 September 2024).

Gers, F.A., Schmidhuber, J. and Cummins, F. (2000) 'Learning to forget: continual prediction with LSTM', *Neural computation*, 12(10), pp. 2451–2471. Available at: https://doi.org/10.1162/089976600300015015.

Graves, A. (2012) 'Supervised Sequence Labelling with Recurrent Neural Networks', 385. Available at: https://doi.org/10.1007/978-3-642-24797-2.

Hochreiter, S. and Schmidhuber, J. (1997) 'Long Short-Term Memory', *Neural Computation*, 9(8), pp. 1735–1780. Available at: https://doi.org/10.1162/NECO.1997.9.8.1735.

Indermühle, E. *et al.* (2011) 'Keyword spotting in online handwritten documents containing text and non-text using BLSTM neural networks', in *Proceedings of the International Conference on Document Analysis and Recognition, ICDAR*, pp. 73–77. Available at: https://doi.org/10.1109/ICDAR.2011.24.

Islam, Md.S. and Mostafa, M.G. (2021) 'Groundwater Status and Challenges in Bangladesh', in, pp. 79–146. Available at: https://doi.org/10.1007/978-3-030-73245-5_4.

Mozer, M.C. (1991) 'Induction of Multiscale Temporal Structure', *Advances in Neural Information Processing Systems*, 4.

Nas, B. and Berktay, A. (2010) 'Groundwater quality mapping in urban groundwater using GIS', *Environmental Monitoring and Assessment*, 160(1–4), pp. 215–227. Available at: https://doi.org/10.1007/S10661-008-0689-4/METRICS.

Nourani, V., Ejlali, R.G. and Alami, M.T. (2011) 'Spatiotemporal groundwater level forecasting in coastal aquifers by hybrid artificial neural network-geostatistics model: A case study', *Environmental Engineering Science*, 28(3), pp. 217–228. Available at: https://doi.org/10.1089/EES.2010.0174.

Nourani, V., Khodkar, K. and Gebremichael, M. (2022) 'Uncertainty assessment of LSTM based groundwater level predictions', *Hydrological Sciences Journal*, 67(5), pp. 773–790. Available at: https://doi.org/10.1080/02626667.2022.2046755.

Oliver, M.A. and Webster, R. (1990) 'Kriging: a method of interpolation for geographical information systems', *International Journal of Geographical Information System*, 4(3), pp. 313–332. Available at: https://doi.org/10.1080/02693799008941549.

Pérez-Ortiz, J.A. *et al.* (2003) 'Kalman filters improve LSTM network performance in problems unsolvable by traditional recurrent nets', *Neural networks : the official journal of the International Neural Network Society*, 16(2), pp. 241–250. Available at: https://doi.org/10.1016/S0893-6080(02)00219-8.

Programme, authorCorporate:UNESCO W.W.A. (2022) 'The United Nations World Water Development Report 2022: groundwater: making the invisible visible', *The United Nations World Water Development Report 2022*, pp. 1–225. Available at: https://unesdoc.unesco.org/ark:/48223/pf0000380721 (Accessed: 12 September 2024).

Rumelhart, D.E., Hinton, G.E. and Williams, R.J. (1986) 'Learning representations by back-propagating errors', *Nature 1986 323:6088*, 323(6088), pp. 533–536. Available at: https://doi.org/10.1038/323533a0.

Shamsudduha, M. (2013) 'Groundwater-fed Irrigation and Drinking Water Supply in Bangladesh: Challenges and Opportunities', in, pp. 150–169.

Sit, M. *et al.* (2020) 'A comprehensive review of deep learning applications in hydrology and water resources', *Water Science and Technology*, 82(12), pp. 2635–2670. Available at: https://doi.org/10.2166/wst.2020.369.

Staudemeyer, R.C. and Morris, E.R. (2019) *Understanding LSTM-a tutorial into Long Short-Term Memory Recurrent Neural Networks*.

Vu, M.T. *et al.* (2020) *Reconstruction of missing groundwater level data by using Long Short-Term Memory (LSTM) deep neural network*.

Werbos, P.J. (1990) 'Backpropagation Through Time: What It Does and How to Do It', *Proceedings of the IEEE*, 78(10), pp. 1550–1560. Available at: https://doi.org/10.1109/5.58337.

Williams, R.J. and Zipser, D. (1989) 'A Learning Algorithm for Continually Running Fully Recurrent Neural Networks', *Neural Computation*, 1(2), pp. 270–280. Available at: https://doi.org/10.1162/NECO.1989.1.2.270.

Yegnanarayana, B. (2009) 'ARTIFICIAL NEURAL NETWORKS (Google eBook)', p. 476. Available at: https://books.google.com/books/about/ARTIFICIAL_NEURAL_NETWORKS.html?id=RTtvUVU_xL4C (Accessed: 13 September 2024).

Yu, Y. *et al.* (2019) 'A review of recurrent neural networks: LSTM cells and network architectures', *Neural computation*, 31(7), pp. 1235–1270.

Zou, J., Han, Y. and So, S.S. (2008) 'Overview of artificial neural networks', *Methods in molecular biology (Clifton, N.J.)*, 458, pp. 15–23. Available at: https://doi.org/10.1007/978-1-60327-101-1_2.